CLINOPYROXENE-MELT TRACE ELEMENT PARTITIONING IN FE- AND AL-RICH BASALTIC SYSTEMS: APPLICATION TO NAKHLITE PETROGENESIS. M. D. Mouser and N. Dygert, Department of Earth and Planetary Sciences, University of Tennessee, Knoxville, TN, 37996 (mmouser@vols.utk.edu)

Introduction: Fe- and Al-rich basaltic systems are prevalent in the Solar System. This work experimentally determines clinopyroxene-melt trace element partitioning in variably aluminous and magnesian ferrobasaltic systems to better understand the partitioning behavior of Fe-rich pyroxenes. The partition coefficients can be applied to understand igneous processes on, and evolution of e.g., Mars, the Moon, and the Angrite parent body.

Among major minerals in planetary interiors, clinopyroxene has a favorable structure to host incompatible trace elements. Clinopyroxene, with a general formula of $(M2)(M1)T_2O_6$, readily hosts trace elements because of the large size of the M2 site in the crystal structure, and the propensity of the mineral for accepting charge balancing coupled substitutions. The M2 site normally houses Ca^{2+} (1.00 Å in 6-fold or 1.12 in 8-fold coordination [1]) and is sizeable enough to fit cations with larger ionic radii e.g., the REEs [e.g., 2-5].

Clinopyroxene-melt trace element partitioning studies have mainly focused on terrestrial-relevant, Mg-rich systems [e.g., 6-9]. These studies have found that in addition to the compositions of the mineral and melt, fO_2, and pressure (P) and temperature (T), substitution of Al onto the tetrahedral site (Al_T), which can charge balance substitution of tri-, tetra-, or pentavalent elements on the M sites, appears to have the largest effect on the trace element partitioning for Mg- and Fe-rich clinopyroxene endmembers. However, Fe-rich systems are understudied and existing data suggests Fe may play a similarly important role [5,10]. Deconvolution of the effects of Al and Fe on trace element partitioning requires experimental investigation. To isolate the controls of Fe and Al we measured pyroxene-melt partition coefficients in high-Fe and low-Al, and low-Fe and high-Al systems.

Methods: *Materials.* Two synthetic base compositions were utilized in this study (Table 1). The compositions are modified versions of an Fe-rich ferrobasalt representative of end-stage lunar magma ocean solidification (FR1290; [11]). An Fe-rich composition was prepared with a very low Al content, and an Al-rich composition was prepared with a lower Fe content, Mg# of ~50. Both compositions were spiked with a REE+HFSE+alkali earth element dopant by about 1 wt% (total). They were ground in an agate mortar for 6 hours before being conditioned to IW-1 in a gas mixing furnace at Brown University.

Experiments. Experiments were conducted using a piston cylinder apparatus at the University of Tennessee in graphite lined Mo capsules. Three successful experiments are presented, one using the Fe-rich endmember (ferrobasalt), one using the Al-rich endmember (intermediate basalt), and one with a 50-50 mixture of the ferrobasalt and intermediate basalt compositions.

	Ferrobasalt	St Dev	Intermediate Basalt	St Dev
SiO_2	34.58	0.57	35.85	0.24
TiO_2	3.68	0.11	2.72	0.04
Al_2O_3	0.49	0.01	5.04	0.39
MgO	1.01	0.03	2.69	0.03
CaO	10.70	0.22	10.35	0.07
MnO	1.10	0.03	0.63	0.02
FeO	44.57	1.04	39.44	0.19
Na_2O	0.10	0.01	0.16	0.02
K_2O	0.16	0.01	0.28	0.01
P_2O_5	0.48	0.01	0.53	0.02
Total	96.88	1.69	97.69	0.21

Table 1. Fe-rich (Ferrobasalt) and Al-rich (Intermediate basalt) compositions in wt% oxide, determined by EMPA analysis of fused and glassed experiments. Glass totals do not include the trace element dopant.

All experiments were conducted at 1 GPa. Experiments were ramped to a superliquidus T (1250–1300°C) and cooled at a rate of 0.1°C/min until reaching the final dwell T (1120–1150°C). Experiments remained at final dwell T for at least 48 hours to approach crystal-melt equilibrium before being isobarically quenched. A representative image of an experiment is shown in Fig.1.

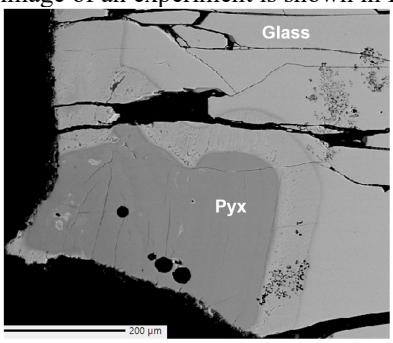

Figure 1. Backscattered electron image of the intermediate basalt experiment. Pyx= clinopyroxene.

Electron Probe Microanalysis (EPMA). Major element analysis and imaging were conducted using a Cameca SX100 electron microprobe at the University of Tennessee. Major elements were analyzed at an accelerating voltage of 15 kV, a beam current of 20nA, and a 2 µm spot size. Pyroxene compositions are presented in Fig. 2.

Laser Ablation Inductively Coupled Plasma Mass Spectrometry (LA-ICP-MS). Trace element data were collected by LA-ICP-MS analysis at the University of Texas at Austin, on the recovered experimental glasses and pyroxene rims using a spot size of 50 µm. Three reference materials were used for the analysis:

NIST612 (primary) and NIST 610 and BCR-2G (secondary). Calculated pyroxene REE partition coefficients are shown in Fig. 3a.

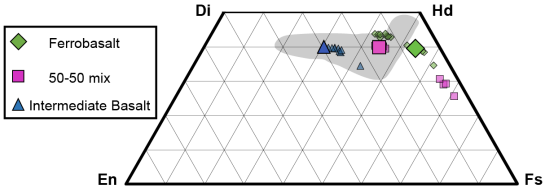

Figure 2. Experimental pyroxene compositions, large symbols on plot denote average rim compositions, small symbols show variability in pyroxene compositions throughout the experiments. Gray region represents Nakhlite clinopyroxene compositions [e.g., 12,13].

Results: Major element compositions of the experimental pyroxenes range from near endmember hedenbergite in the case of the Al-poor ferrobasalt composition, to an intermediate Di-Hd in the more aluminous intermediate composition (Fig. 2). Calculated partition coefficients show that the Al-poor pyroxenes in the ferrobasalt least favor REEs among the three experiments, and the Al-rich pyroxenes in the intermediate composition most favor REEs (Fig. 3a). The pyroxenes all show the general trend of being more enriched in HREEs as compared to LREEs, with the exception of Eu. The Al-rich experiment has a slight negative Eu anomaly, while the Fe-rich and mix experiments show positive Eu anomalies with the former being strongly positive in comparison.

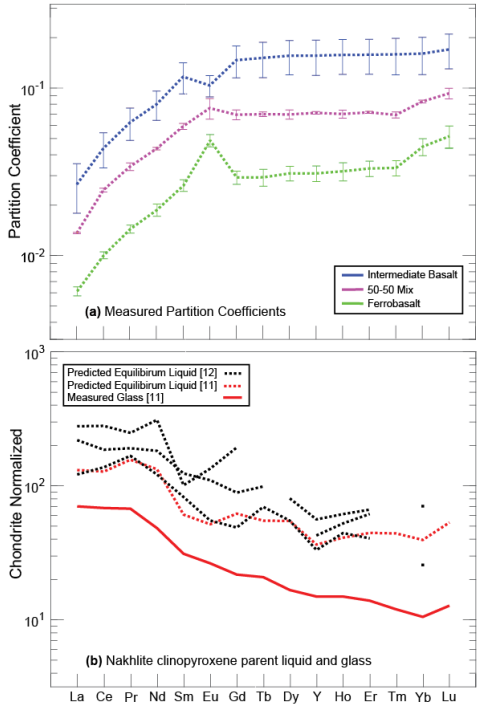

Figure 3. Experimentally determined partition coefficients (a), predicted nakhlite equlibirum liquid compositions with a glass measurement for reference (b). Nakhlite data are from [12,13].

Discussion: A notable difference among the samples is their Eu anomalies, which are related to partitioning of Eu into the clinopyroxene structure as well as the partitioning behavior of neighboring REEs. The Al-rich intermediate experiment exhibits a small negative anomaly, likely owing to the coupled substitution of $Ca^{2+} + Si^{4+} \leftrightarrow REE^{3+} + Al^{3+}$, while Eu is dominantly in the 2+ valence state at the low fO_2s. The Al-poor ferrobasaltic experiment (and to a lesser extent the 50-50 mix experiment) exhibits positive Eu anomalies owing to the relative lack of Al^{3+} to facilitate coupled substitution with the REE^{3+}. We note that positive correlation of U, Th, and HFSEE partition coefficients with Al also suggest their substitutions coupled with Al_T.

These experiments have important implications for the evolution of Fe-rich magmatic systems, such as the Martian lava flow that nakhlites are believed to have originated from [12,14]. The partition coefficients from the Al-rich (intermediate basalt) experiment may be used to calculate the equilibrium liquid from which the nakhlite pyroxene rims formed, as their major element compositions are similar. The equilibrium liquid can then be compared to the coexisting glass composition to infer the evolution of the trace element chemistry during the nakhlite crystallization process. Fig. 3b shows that the equilibrium liquid is higher in REEs then the measured coexisting glass. This suggests the coexisting glasses are not in equilibrium with the clinopyroxene compositions, implying that the clinopyroxene parent liquids were physically separated from the crystals by settling and/or compaction of the parent liquids out of a crystal mush in a cumulate pile. Alternatively, the discrepancy may be related to differences in the nakhlite crystallization *T* and experimental *Ts*. Future experiments will be conducted at different *P-T* conditions to further constrain trace element partitioning relationships in Al-Fe-rich systems, to understand the formation of the nakhlites, and trace element evolution in Fe-rich systems in general.

References: [1] Shannon, R. D. (1976) *Acta Cryst. A32,* 751-767. [2] Cameron M. and Papike J. J. (1981) *Am. Min., 66,* 1-50. [3] McKay G. et al. (1986) *GCA, 50,* 927-937. [4] Gallahan W. E. and Nielsen R. L. (1992) *GCA, 56*, 2387-2404. [5] Olin P. H. and Wolff J. A. (2010) *Contrib. Min. Pet., 160*, 761-775. [6] Gaetani G. A. and Grove T. L. (1995) *GCA, 59*, 1951-1962. [7] Sun C. and Liang Y. (2012) *Contrib. Min. Pet., 163*, 807-823. [8] Sun C. and Liang Y. (2013) *Chem. Geology, 358*, 23-36. [9] Sun C. et al. (2017) *GCA, 206*, 273-295. [10] Dygert N. et al. (2014) *GCA, 132*, 170-186. [11] Longhi J. (2003) *JGR, 180*, 5083. [12] Day, J. M. D. et al. (2006) *MAPS*, *41,* 581-606. [13] Udry, A. et al. (2012) *MAPS, 47,* 1575-1589. [14] Treiman, A. H. (2005) *Chemie der Erde, 65,* 203-270.